NANO LETTERS

2005
Vol. 5, No. 12
2389−2393

Determination of the Bending Modulus of an Individual Multiwall Carbon Nanotube using an Electric Harmonic Detection of Resonance Technique

R. Ciocan, J. Gaillard, M. J. Skove, and A. M. Rao*

Department of Physics and Astronomy, Clemson University, Clemson, South Carolina 29634

Received July 27, 2005; Revised Manuscript Received November 3, 2005

ABSTRACT

We report a new method of measuring the amplitude and phase of oscillations of individual multiwall carbon nanotubes (MWNTs). As in many other experiments, we excite the oscillations electrostatically, but we show that we can detect the amplitude and phase of the resulting oscillation electrically. As an example, we present measurements of the fundamental and first two overtones of the diving board resonance of a MWNT at 0.339, 2.42, and 5.31 MHz in ambient conditions. The corresponding quality factors were 67, 36, and 25.

There is extensive experimental and theoretical interest in the mechanical properties of carbon nanotubes. This is due, in part, to the presence of strong covalent bonds in these nearly 1D structures. The first experimental determination of the bending modulus (E_b) for an individual MWNT used the intrinsic thermal vibrations analyzed under a transmission electron microscope (TEM)[1]. Wong et al.[2] measured the lateral force needed to bend a MWNT clamped at one end, while Yu et al.[3] measured the stress−strain curves for individual MWNTs clamped between two atomic force microscope (AFM) cantilevers inside a scanning electron microscope (SEM). Cooling-induced compressive deformation of MWNTs embedded in an epoxy matrix was monitored in a temperature-dependent micro-Raman study[4]. Finally, E_b has also been determined from electric-field-induced mechanical oscillations in cantilevered MWNTs from the amplitude-frequency response recorded using the following: (i) a TEM,[5] (ii) an SEM,[6] (iii) field-emission microscopy,[7] and (iv) an optical microscope.[8,9]

Despite all of the above different means of measuring the resonances of MWNTs, we have found no reports of measuring the oscillations of a cantilevered nanotube electrically. This desired goal would allow the simple determination of the resonance frequency of cantilevers built into integrated circuits or cantilevers whose response can be monitored as a function of temperature and pressure. We have found that it is possible to make measurements of the higher harmonics of the charge induced on a cantilevered MWNT. In particular, the second harmonic provides a measure of the mechanical resonances with good signal-to-noise ratio.

A schematic of our measurement setup is shown in Figure 1a. A MWNT is first placed on a sharpened gold-coated tungsten probe tip by applying a dc voltage between the coated tungsten probe and a mat of MWNTs attached to SEM tape. Occasionally, an individual MWNT attaches to the tip.[9] Another gold-coated tungsten probe tip serves as the counter electrode and is brought in close proximity to and aligned with the MWNT (Figure 1b). The alignment of the MWNT with the counter electrode was monitored carefully using a dark field optical microscope (Nikon Epiphot 200) equipped with a digital camera (MOTICAM 1000). An ac voltage, V_{ac}, as well as a dc voltage, V_{dc}, induce charges on the MWNT.[5] The electrostatic force, F_e, between the charges residing on the MWNT and the counter electrode causes the MWNT to oscillate (Figure 1c). When $V_{ac} = 0$, the total potential difference between the MWNT and the counter electrode is $(W_{Au} - W_{MWNT})/e + V_{dc}$, where W_{Au} and W_{MWNT} are the work functions for the counter electrode and the MWNT. The modulated charge on the MWNT is detected and amplified by the low noise charge amplifier labeled LNA in Figure 1a (Amptek A250). Finally, the output signal of the LNA is detected coherently using a lock-in amplifier set for 2nd harmonic detection. We find a higher signal-to-noise ratio using detection at the 2nd harmonic rather than detection at the same frequency as the oscillator. We attribute this to avoiding the much larger interfering signal at the driving frequency. All of the measurements reported in this Letter were performed in air under ambient conditions. A comput-

* Corresponding author. E-mail: arao@clemson.edu.

10.1021/nl0514644 CCC: $30.25
Published on Web 11/18/2005

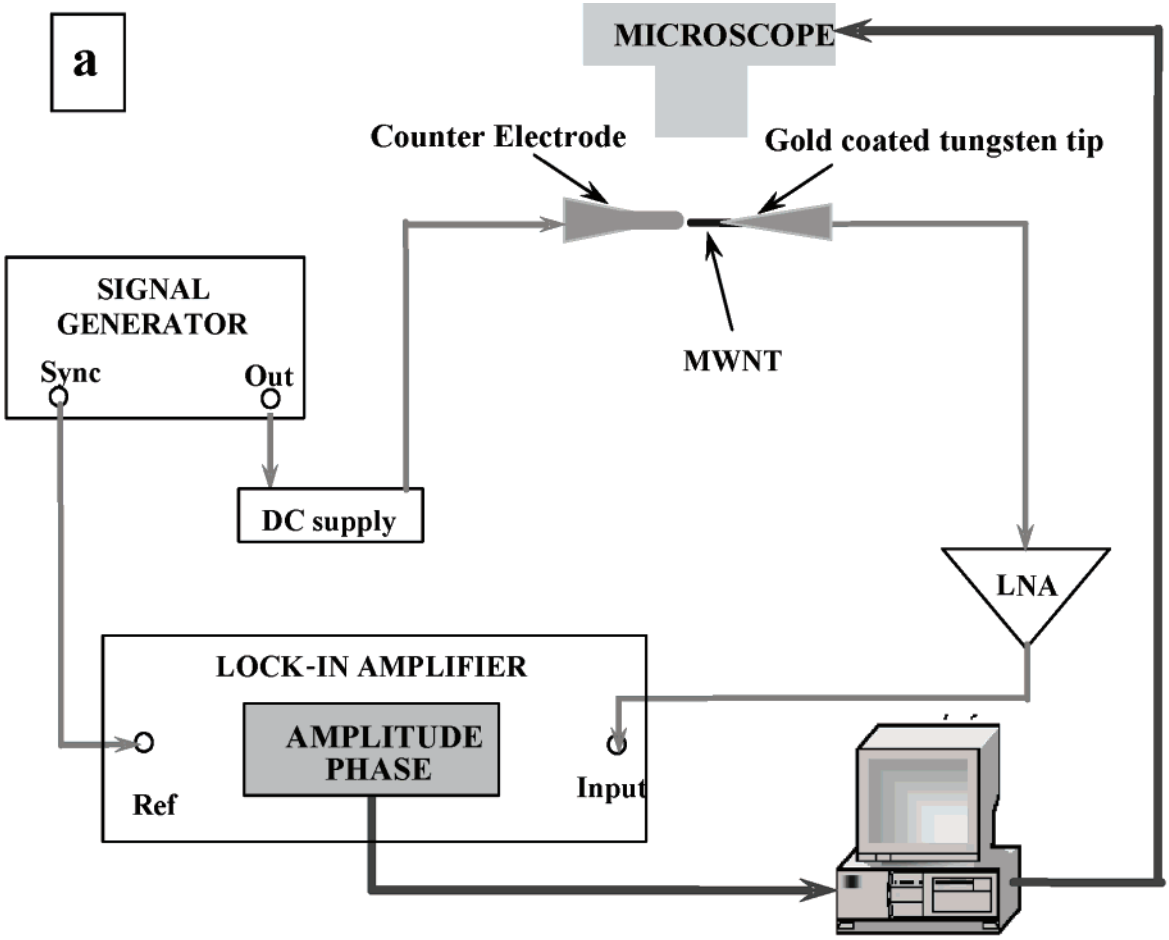

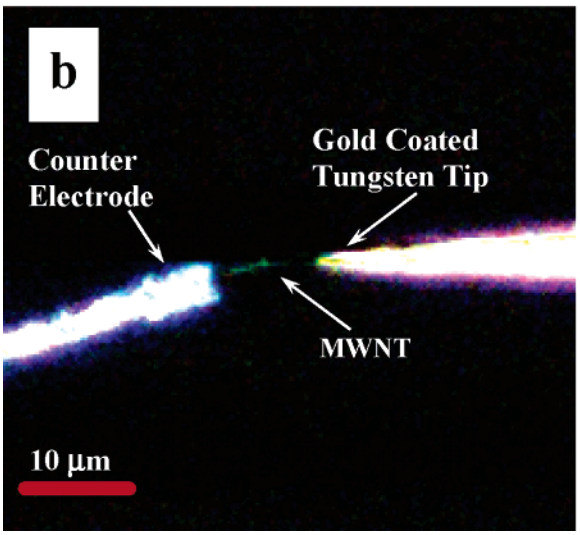

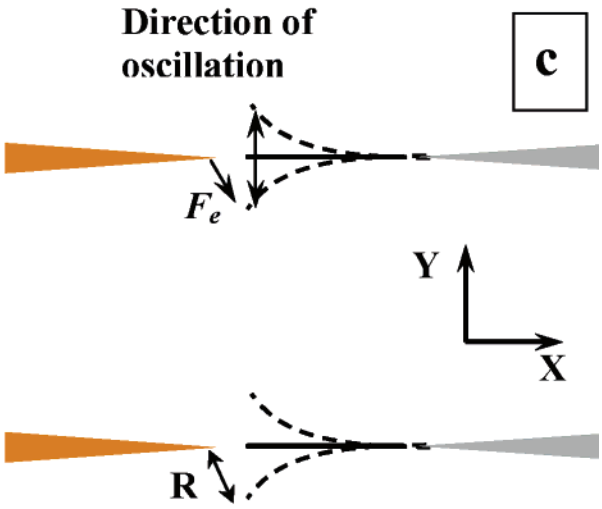

Figure 1. (a) Experimental setup for harmonic detection of electrically induced mechanic resonance in an individual multiwall carbon nanotube (MWNT). (b) Dark field microscope image of the geometrical setup for the MWNT and the counter electrode assembly. The MWNT is in very close proximity of the counter electrode (see text). (c) A schematic of mechanical oscillations induced in a MWNT by the electric force, F_e, when the MWNT and the counter electrode are separated by a distance R.

erized data acquisition system collected the excitation frequency (f_E) provided by the signal generator and the amplitude and phase of the LNA output signal as measured by the lock-in amplifier. The system described in Figure 1a was tested by comparing the resonance frequencies of a typical silicon cantilever (90 μm long, 35 μm wide, and 2 μm thick) using a commercial AFM (Veeco CP II). The resonant frequency of the Si cantilever as determined using our method, and the optical method of an AFM were 323 and 326 kHz, respectively. This comparison confirmed that

our system (using electrical detection of mechanical resonances) provides resonance frequencies in good agreement with those obtained using the AFM by optical detection of resonances.

The charges accumulated at the tip of the MWNT and on the counter electrode can be assumed to be quasi point charges, Q, which can be expressed as[10]

$$Q = \alpha[(W_{Au} - W_{MWNT}) + e(V_{dc} + V_{ac}\cos 2\pi f_E t)] \quad (1)$$

where α is a geometrical factor related to the counter electrode geometry and the charges are separated by a distance R (Figure 1c). The Coulomb force, F_e, between the charges on the counter-electrode tip and MWNT is given by

$$F_e = \frac{1}{4\pi\epsilon_o\epsilon_r R^2} Q^2 = \frac{\alpha^2}{4\pi\epsilon_o\epsilon_r R^2}[A_{DC} + A_{f_E}\cos 2\pi f_E t + A_{2f_E}\cos 4\pi f_E t] \quad (2)$$

where $A_{DC} = [(W_{Au} - W_{MWNT}) + eV_{dc}]^2 + e^2(V_{ac}^2/2)$; $A_{f_E} = 2eV_{ac}[(W_{Au} - W_{MWNT}) + eV_{dc}]$ and $A_{2f_E} = e^2(V_{ac}^2/2)$. Typical experimental parameters V_{dc}, V_{ac}, and R were 9 V, 5 V (peak to peak), and 200 nm, which resulted in small oscillations of the MWNT not observable in the optical microscope, presumably along the y direction. For small oscillations, the excitation, y, of each normal mode can be expressed[11] as a forced oscillator with damping $b(\partial y/\partial t)$

$$m_e\frac{\partial^2 y}{\partial t^2} + b\frac{\partial y}{\partial t} + k_e y = F_e \quad (3)$$

where m_e, k_e, and F_e are the mass, elastic constant, and force for an equivalent oscillator driven at frequency f_E. When the resonance frequency, f_i, of a mode is near f_E, the steady-state solution for eq 3 can be written as

$$y = \frac{\alpha^2}{4\pi\epsilon_o\epsilon_r R^2}\frac{A_{f_E}}{2\pi\sqrt{m_e^2(f_E^2 - f_i^2)^2 + b^2 f_E^2}}\sin(2\pi f_E t - \delta) \quad (4)$$

where the phase shift, δ, for the mode with frequency f_i is given by

$$\delta = \cos^{-1}\left(\frac{bf_E}{\sqrt{m_e^2(f_E^2 - f_i^2)^2 + b^2 f_E^2}}\right) \quad (5)$$

The resonance frequencies of the cantilevered MWNT are obtained by finding the excitation frequencies that match natural mode frequencies. Note that similar expressions can be obtained for a steady-state solution when f_E is near $^1/_2$ f_i.

Figure 2a shows typical resonance spectra for a CVD grown MWNT with $L = 10$ μm, $D_i = 17$ nm, and $D_o = 57$ nm.[12] The initial gap distance R_i (i.e., $V_{ac} = V_{dc} = 0$) is estimated to be ~200 nm, which is the resolution limit of our optical system. In accord with eqs 4 and 5, f_i for the MWNT is identified with the frequency for which the amplitude reaches its local maximum (Figure 2a, light circle trace). The light triangle trace in Figure 2a shows the associated 160° change in δ. The amplitude (dark circles)

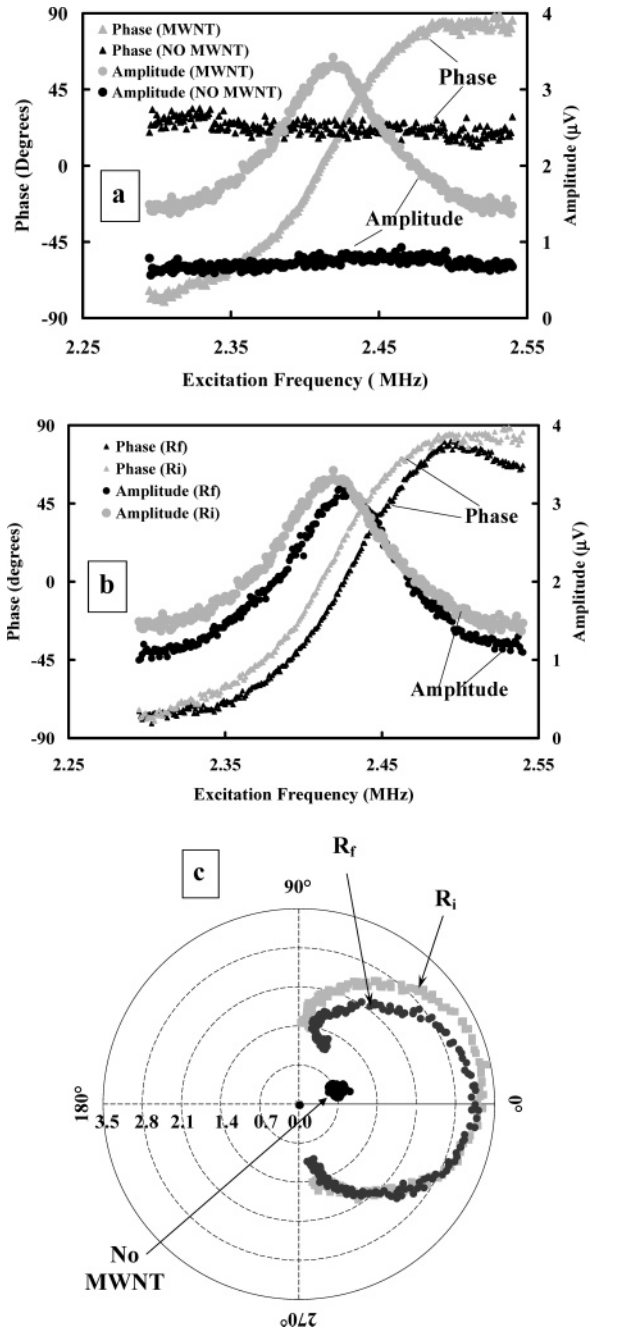

Figure 2. (a) Frequency dependence for the amplitude (circles) and phase (triangles) signals obtained from the output of the lock-in amplifier in the presence (light) and absence (dark) of a MWNT. (b) The amplitude (circles) and phase (triangles) signals plotted as a function of frequency for two different distances of the MWNT from the counter electrode: R_i (light), R_f (dark) where $R_f > R_i$. (c) A polar plot (where the radius is the amplitude and the angle is the phase) of the data presented for the two resonances shown in Figure 2b. As expected from theory, the plot is a circle displaced from the origin by the background signal. The resonance frequency is determined to be at the place on the circle where the distance between data points on the circle is a maximum.

and phase (dark triangles) signals obtained for the same geometry of the electrodes in the absence of the MWNT are also plotted in Figure 2a. The maximum amplitude and phase change occur when the excitation frequency reaches 2.420 MHz. No noticeable changes in the traces for the amplitude and phase can be discerned in the frequency range between 2.250 and 2.550 MHz when the MWNT is absent.

As a further verification that the local maximum observed using electrical detection of resonance in the cantilevered MWNT corresponds to a resonance frequency of the MWNT, we remeasured f_i and δ after moving the manual micromanipulator to increase R. The motion was less than the resolution of the optical system, so we estimate the difference between R_i and R_f to be less than 200 nm. It is not essential for our method to know the exact change in order to show qualitatively that increasing R increases f_i. Figure 2b depicts the results for two gap distances: R_i and $R_f > R_i$. The frequency shifts from 2.420 to 2.425 MHz in the amplitude traces (Figure 2b), but the polar plot (Figure 2c), which involves both the amplitude and phase, shows that the actual shift is from 2.420 to 2.436 MHz. The slight increase of f_i when R is increased (i) confirms that the resonance data shown in Figure 2 corresponds to a mechanical resonance of the cantilevered MWNT and (ii) provides evidence for parametric and/or nonlinear effects.[5,6,13] Furthermore, the phase change remains constant (around 160°) when the distance R is varied, also consistent with eq 5. Finally, it should be mentioned that the quality factor, which is a measure of how mechanical energy is transferred into electric energy, decreases from 37 to 31 when R increases (see Figure 2b).

For a MWNT clamped at one end, the frequency of the ith mode of vibration is given by[5,14,15]

$$f_i = \frac{\beta_i^2}{8\pi}\frac{1}{L^2}\sqrt{\frac{(D_o^2 + D_i^2)E_b}{\rho}} \qquad (6)$$

where L is the tube length, D_o and D_i are the outer and inner tube diameters, respectively. ρ is the density of the MWNT and the β_i values are determined from the boundary conditions to be $\beta_1 = 1.875$, $\beta_2 = 4.694$, and $\beta_3 = 7.855$.[14] We measured the density, ρ, of MWNTs to be $\rho = 2100$ Kg/m^3.[16] Note that we measure the bending modulus of the nanotube. As long as the nanotube does not change its geometry by buckling[5] or any other such deformation, the bending modulus is equal to Young's modulus.[15] The length and outside diameter for the MWNT whose resonance spectra are discussed in Figure 2 were determined from scanning electron microscope images to be: $L = 10$ μm, $D_o = 57$ nm, and the inner diameter was determined numerically using the algorithm described below. In an independent experiment, the resonance spectra for another MWNT were measured electrically and its L, D_o, and D_i values were determined using transmission electron microscopy. Table 1 summarizes the measurements performed on these two MWNTs.

The resonances determined experimentally for the MWNT discussed in Figure 2 were found at $f_{1e} = 0.339$ MHz, $f_{2e} = 2.42$ MHz, and $f_{3e} = 5.31$ MHz (Figure 3a and b). The

Table 1. Geometric Parameters of the MWNTs Investigated in This Study[a]

sample	L (μm)	D_o (nm)	D_i (nm)	f_{1e} (MHz)
1	10	57	17	0.34
2	8.9	86.6	11.4	0.45

[a] L, D_o, D_i, and f_{1e} correspond, respectively, to the length, outer and inner tube diameters, and the fundamental resonant frequency.

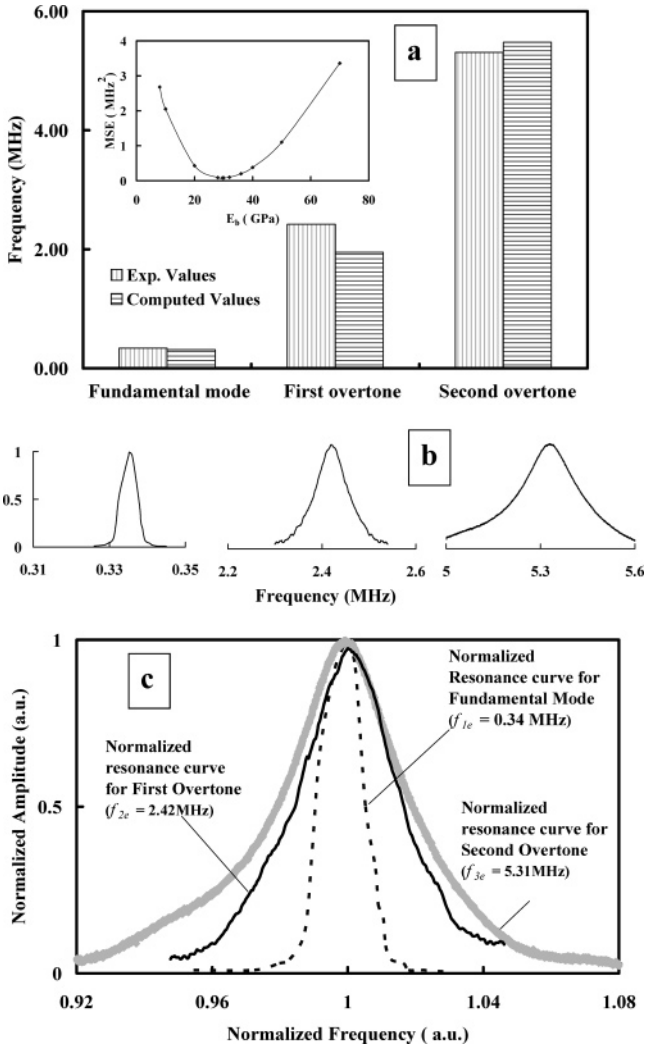

Figure 3. (a) Experimental (vertical stripes) and computed (horizontal stripes) frequencies for the fundamental, first, and second overtones in a MWNT. The inset is a plot of the mean squared error between the experimental and computed values for the bending modulus (see the text). (b) The measured amplitude for the fundamental, first, and second overtones in a MWNT. For clarity, these amplitudes are plotted on a normalized ordinate. (c) Same as b but plotted on a normalized frequency scale.

bending modulus, E_b, was computed using a multistep procedure. At each step, the f_i values were computed using eq 6 starting with the measured values for D_o, D_i, and L and a range of values for E_b. Then the mean squared error (MSE) for a particular E_b was computed as

$$\mathrm{MSE} = \frac{1}{3}\sum_{i=1}^{3}(f_i - f_{ie})^2 \qquad (7)$$

As the inset in Figure 3a shows, we find a minimum in MSE for $E_b = 29.6$ GPa. Then, the values of L and D_o were perturbed by about $\pm 10\%$, and the minima in MSE were recomputed to ensure ourselves that the minimum was global rather than local. A comparison between frequencies determined experimentally (vertical stripes) and computed values (horizontal stripes) for $E_b = 29.6$ GPa is also shown in Figure 3a. The average error in frequency estimation is about $\sim 10\%$ (ranging from 18% for the first overtone to 3% for the second overtone). Our value for the bending modulus $E_b = 29.6 \pm 2.9$ GPa is in excellent agreement with those reported in the literature for MWNTs with comparable dimensions.[5] The quality factor for each of the three resonances is 67, 36, and 25 for the fundamental and first two overtones, respectively (see Figure 3c). Recently, a doubly clamped single-walled carbon nanotube was actuated electrically and its resonant frequency was detected using a mixer technique by McEuen and co-workers.[17] Although their technique is valuable for a beam in a guitar-like configuration, it cannot be applied to a cantilevered nanostructure. Our values for the quality factor compare well with the quality factors $\sim 10-40$ reported in the doubly clamped geometry at room temperature and low pressure (less than 10 Torr).

In conclusion, we describe a method for exciting and measuring the resonance frequencies of an individual MWNT electrically. Our method detects the resonance using higher harmonics of the exciting frequency and provides both the amplitude and phase information. As a first application of our technique, we obtain a bending modulus of 29.6 GPa from the three resonances observed experimentally using an iterative algorithm. This bending modulus is in excellent agreement with those reported in the literature from stress−strain measurements of MWNTs with comparable dimensions. This fully electrical approach for exciting and measuring the resonance frequencies is convenient and advantageous in devices that use MWNTs as the circuit elements or detectors.

References

(1) Treacy, M. M. J.; Ebbesen, T. W.; Gibson, J. M. *Nature* **1996**, *381*, 678.
(2) Wong, E. W.; Sheehan, P. E.; Lieber, C. M. *Science* **1997**, *277*, 1971.
(3) Yu, M.; Lourie, O.; Dyer, M. J.; Moloni, K.; Kelly, T. F.; Ruoff, R. S. *Science* **2000**, *287*, 637.
(4) Lourie, O.; Wagner, H. D. *J. Mater. Res.* **1998**, *13*, 2418.
(5) Poncharal, P.; Wang, Z. L.; Ugarte, D.; de Heer , W. A. *Science* **1999**, *283*, 1513.
(6) Yu, M.; Wagner, G. J.; Ruoff, R. S.; Dyer, M. J. *Phys. Rev. B* **2002,** *66*, 073406.
(7) Purcell, S. T.; Vincent, P.; Journet, C.; Vu Thien Binh *Phys. Rev. Lett.* **2002**, *89*, 276103.
(8) Yum, K.; Wang, Z.; Suryavanshi, A. P.; Yu, M. *J. Appl. Phys.* **2004**, *96*, 3933.
(9) Gaillard, J.; Skove, M. J.; Rao, A. M. *Proc. Mater. Res. Soc.* Meeting, Boston, MA, 2004.
(10) Gao, R.; Pan, Z.; Wang, Z. L. *Appl. Phys. Lett.* **2001**, *78*, 757.
(11) Main, I. G. *Vibration and Waves in Physics*; Cambridge University Press: Cambridge, U.K., 1993; p 59.
(12) Gaillard, J.; Skove, M. J.; Rao, A. M. *Appl. Phys. Lett.* **2005**, *86*, 233109.
(13) Sarid, D. *Scanning Force Microscopy: With Applications to Electric, Magnetic, and Atomic Forces*; Oxford University Press: New York, 1991; p 142.
(14) Wang, Z. L.; Poncharal, P.; de Heer, W. A. *Pure Appl. Chem.* **2000**, *72*, 209.
(15) Qian, D.; Wagner, G. J.; Liu, W. K.; Yu, M.; Ruoff, R. S. *Appl. Mech. Rev.* **2002**, *55*, 495.
(16) Lu, Q.; Keskar, G.; Ciocan, R.; Larcom, L. L.; Rao, A. M. *NT05: Sixth International Conference on the Science and Application of Nanotubes*; Gothenburg, Sweden, 2005; p 426.
(17) Sazonova, V.; Yaishm, Y.; Üstünel, H.; Roundy, D.; Arias, T.; McEuen, P. *Nature* **2004**, *431*, 284.

NL0514644